Contents lists available at SciOpen

Food Science and Human Wellness

journal homepage: https://www.sciopen.com/journal/2097-0765

China Food Publishing Co.

Agrocybe cylindracea polysaccharides repair the intestinal mucosal barrier in DSS-induced colitis by modulating the gut microbiota -macrophage axis

Zaoxuan Wu[a,b], Shujian Wu[c,d], Xiuying Liu[a,b], Shuze Chen[a,b], Senbao Xu[a,b], Yunying Gong[a,b], Qiujuan Ye[a,b], Xuefeng Gao[c,d], Ye Chen[a,c,d,*]

[a] *Department of Gastroenterology, Guangdong Provincial Key Laboratory of Gastroenterology, State Key Laboratory of Organ Failure Research, Nanfang Hospital, Southern Medical University, Guangzhou 510000, China*
[b] *The First School of Clinical Medicine, Southern Medical University, Guangzhou 510000, China*
[c] *Department of Gastroenterology, Shenzhen Hospital, Southern Medical University, Shenzhen 518000, China*
[d] *Integrative Clinical Microecology Center, Shenzhen Key Laboratory of Gastrointestinal Microbiota and Disease, Shenzhen Clinical Research Center for Digestive Disease, Shenzhen Technology Research Center of Gut Microbiota Transplantation, Shenzhen Hospital, Southern Medical University, Shenzhen 518000, China*

ARTICLE INFO

Article history:
Received 4 June 2024
Received in revised form 23 September 2024
Accepted 19 November 2024

Keywords:
Agrocybe cylindracea polysaccharides
Ulcerative colitis
Gut microbiota
M2 macrophage polarization
Intestinal mucosal barrier

ABSTRACT

The *Agrocybe cylindracea* polysaccharides (ACP) have been shown to possess various health benefits. However, the anti-inflammatory effects of ACP and the mechanisms underlying these effects remain poorly understood. In this study, we delved into the potential of ACP in mitigating colitis induced by dextrose sodium sulfate (DSS) in C57BL/6J mice and explored the associated mechanisms. ACP demonstrated notable anti-inflammatory effects in the intestines, as evidenced by the restoration of various indicators such as increased body weight and colon length, decreased disease activity index (DAI) score, and alleviation of pathological damage in the colon. Additionally, ACP upregulated the expression of ZO-1, Occludin, and Muc2, suggesting a restoration of the mechanical and mucus barriers of the intestinal mucosa. Furthermore, ACP facilitated the polarization of M2 macrophages and preserved intestinal immune balance. The impact of ACP on the biological barrier was further scrutinized. ACP ameliorated disruptions in the gut microbiota, particularly by enhancing the relative abundance of bacteria that produce short-chain fatty acids (*Anaerostipes*, *Romboutsia*, and *Butyricicoccus*). Remarkably, the ameliorative effects of ACP on colitis were compromised upon the removal of the microbial community, but were restored post fecal microbiota transplantation (FMT), indicating that the efficacy of ACP in alleviating colitis is dependent on the gut microbiota. Intriguingly, the regulatory influence of ACP on macrophages also hinged on the gut microbiota. In essence, ACP exhibits the potential to modulate the composition of the gut microbiota, fostering the growth of beneficial bacteria, which in turn promotes the polarization of colonic M2 macrophages and facilitates the repair of the intestinal mucosal barrier in DSS-induced colitis. These findings underscore the capacity of ACP to enhance the intestinal mucosal barrier and ameliorate colitis by modulating the gut microbiota-macrophage axis, suggesting that ACP could serve as a functional food supplement for preserving intestinal homeostasis and preventing colitis.

1. Introduction

Inflammatory bowel disease (IBD) is an intestinal disorder characterized by chronic inflammation of unknown etiology, impacted by host genetics, immunity, diet, and gut microbiome[1]. With the changes of living environment and dietary habits, the global incidence of IBD has reached 0.3% and is increasing[2]. Most therapeutic agents used to treat IBD, such as 5-aminosalicylic acid, corticosteroids and immunosuppressants, as well as surgical treatments, are associated with serious side effects in extreme cases, including allergic reactions and intolerance[3]. Therefore, there is still an urgent need to develop effective and safe therapeutic agents.

Intestinal mucosal barrier, including mechanical barrier, chemical barrier, and immune barrier, plays a key role in the pathogenesis

* Corresponding author at : Department of Gastroenterology, Guangdong Provincial Key Laboratory of Gastroenterology, State Key Laboratory of Organ Failure Research, Nanfang Hospital, Southern Medical University, Guangzhou 510000, China .
E-mail address : yechen_fimmu@163.com (Y. Chen)
Peer review under responsibility of Beijing Academy of Food Sciences.

SciOpen Publishing services by Tsinghua University Press

http://doi.org/10.26599/FSHW.2024.9250440

of IBD[4]. Increasing evidences revealed that dysbiosis of the intestinal microbiota may lead to impaired intestinal mucosal barrier function, which in turn triggers intestinal inflammation. Intestinal immune disorders are another major pathogenesis of IBD, in which macrophages are key cells in intestinal innate immunity[5]. Notably, it has been reported that changes in the gut microbiota can affect the polarization state of macrophages, thereby disturbing the balance of the intestinal immune system[6]. Therefore, the interaction between gut microbiota and macrophages plays a critical role in the repairment of intestinal mucosal barrier in IBD. In-depth study of this interaction may provide an important basis for developing new target and treatment strategies for IBD patients.

Dietary intervention is considered to be a key regulatory modality affecting gut microbiota and intestinal immunity[7-8]. Previous studies have revealed that several polysaccharides from diet can protect the intestinal mucosal barrier and maintaining the balance of the gut microbiota and intestinal immunity[9-10]. Research on edible fungi polysaccharides (EFPs) have shown potential benefits in regulating gut microbiota[11] and intestinal immunity[12]. *Agrocybe cylindracea* (AC), as a common edible mushroom for daily consumption, are high in polysaccharides (about 70%) and are an important source of active EFPs[13]. However, there are few studies on *A. cylindracea* polysaccharides (ACP) can alleviate impairment of intestinal mucosal barrier in colitis. Thus, the objective of this study was to obtain polysaccharides from AC and subsequently investigate the effect of ACP on dextrose sodium sulfate (DSS)-induced colitis. Furthermore, the possible mechanism based on the interactions between gut microbiota and macrophages was analyzed.

2. Materials and methods

2.1 Preparation and compositional analysis of ACP

2.1.1 Preparation of ACP

AC was obtained from Guangdong YueWei Technology Co., Ltd. (Guangzhou, China). The freshly dried AC solids were ground into powder using a high-speed pulverizer and then passed through a 100 meshes sieve. The AC powder was heated with distilled water (1:20, *m/V*) in a water bath at 90 ℃ for 4 h and then centrifuged to retain the supernatant. Then added 2-fold volume of anhydrous ethanol to the supernatant and kept at 4 ℃ for 2 h. The precipitate was collected by centrifugation (4 ℃, 4 000 r/min, 15 min) and dissolved in distilled water to obtain crude ACP. Sevage reagent (chloroform:*n*-butanol = 4:1, *V/V*) was added to the crude ACP solution and shaken violently to remove free proteins. After continuous dialysis (cut-off value 7 000 Da) at 4 ℃ for 24 h, the resulting retentate was freeze-dried to obtain purified ACP. A total of 400 g of AC was used and 19.04 g of ACP was finally obtained, which means that the yield of ACP was 4.76%.

2.1.2 Molecular weight (Mw) determination of ACP

ACP was dissolved in 0.1 mol/L $NaNO_3$ aqueous solution (containing 0.02% NaN_3, *m/m*) at the concentration of 1 mg/mL, and then filtered through a filter of 0.45 m pore size for further detected. A DAWN HELEOS-II laser photometer (Wyatt Technology Co., CA, USA) equipped with two tandem columns (300 mm × 8 mm, Shodex OH-pak SB-805 and 803; Showa Denko K.K., Tokyo, Japan) was used for detection. The flow rate was 0.6 mL/min. Finally, the Mw of each component was calculated using data from a differential refractive index detector (Optilab T-rEX, Wyatt Technology Co., CA, USA).

2.1.3 Monosaccharide composition of ACP

ACP was acid-hydrolyzed to monosaccharides by adding trifluoroacetic acid (2 mol/L). An ion chromatography system (ICS 5000+, Thermo, MA, USA) was used. A liquid chromatography column, Dionex™ CarboPac™ PA20 (150 mm × 3.0 mm, 10 μm), was selected and eluted at a flow rate of 0.5 mL/min, while the monosaccharide fractions were analysed and detected using an electrochemical detector.

2.1.4 Fourier transform infrared spectroscopy (FT-IR) analysis of ACP

A total of 20 mg ACP was mixed with 200 mg KBr, and then pressed into 1 mm pellets to be detected. FT-IR (Nicolet iZ-10, Thermo, MA, USA) was used for scanning and analysis in the range of 4 000 to 400 cm^{-1}. Finally, the infrared absorption spectrum of the transmittance of ACP with wave number was obtained.

2.1.5 Electron microscope scanning of ACP

The ACP sample, coated with a thin gold layer, were placed on the substrate, and then observed and photographed using a scanning electronic microscope (Zeiss Merlin Compact, Oberkochen, Germany).

2.2 Animal experiments

2.2.1 Animals

Wild-type male C57BL/6 mice, aged 6–8 weeks old, were purchased from Beijing Sipeifu Biotechnology Company. Mice were acclimatized at (22 ± 2) °C, (50 ± 5)% humidity, and 12 h light-dark cycle for one week in a specific pathogen-free (SPF) environment. During the experiment, the mice were weighed and their stool characteristics were evaluated daily. At the end of modelling, all mice were euthanised after pentobarbital anaesthesia. Colon tissue and cecum contents from mice were collected immediately and stored at –80 °C or fixed in 4% paraformaldehyde for subsequent experiments. All animal experiments complied with the ARRIVE guidelines and be carried out in accordance with the U.K. Animals (Scientific Procedures) Act, 1986 and associated guidelines, EU Directive 2010/63/EU for animal experiments, or the National Institutes of Health guide for the care and use of Laboratory animals (NIH Publications No. 8023, revised 1978). All animal experimental protocols in this study have been confirmed and approved by The Institutional Animal Care and Use Committee of Southern Medical University, China (SMUL2022289).

2.2.2 DSS-induced colitis mice model and ACP treatment of mice

The mice were randomly divided into 4 groups: control group, DSS group, DSS + high-ACP group (300 mg/kg·day ACP), and DSS + low-ACP group (100 mg/kg·day ACP). The modelling procedure is shown in Fig. 2A, where mice in the control and DSS groups were given 200 μL of PBS by gavage daily; whereas mice in the DSS + high-ACP group and the DSS + low-ACP group were gavaged with 200 μL of PBS containing 300 mg/kg ACP and 100 mg/kg ACP once daily for 14 days, respectively. On days 8 to 14, mice in all groups except the control group were given 2.5% (*m/V*) DSS (36–50 kDa, MP Biomedicals, CA, USA) in drinking water to induce colitis.

2.2.3 Depletion of gut microbiota by antibiotic cocktail

Mice were administered with an antibiotic cocktail consisting of ampicillin (1 g/L), neomycin (1 g/L), metronidazole (1 g/L), and vancomycin (0.5 g/L) dissolved in drinking water for 7 days. At the same time, the mice were also given a daily gavage of the cocktail (vancomycin 100 mg/kg·day, metronidazole 200 mg/kg·day, neomycin 200 mg/kg·day, and ampicillin 200 mg/kg·day) to further deplete the gut microbiota. Depletion of the gut microbiota was confirmed by collecting faecal samples for bacterial plate smears. This was followed by ACP treatment and induction of experimental colitis as described above.

2.2.4 Fecal microbiota transplantation (FMT)

Donor mice were randomly divided into 3 groups: control group, DSS group and ACP group. The DSS group received 2.5% DSS induced colitis for 7 days, and the ACP group received ACP (300 mg/kg·day) daily, and the fecal samples were collected during the last 3 days of the experiment. The feces were made up to a concentration of 50 mg/mL with sterile normal saline, and swirled in an oscillating vortex for 5 min. After filtration by a 70 μm filter, the feces were centrifuged at high speed (4 ℃, 10 000 r/min, 5 min) and then the precipitates were re-suspended with sterile normal saline containing 30% glycerol to prepare bacterial solution for transplantation. Receptor mice were also divided into 3 groups: DSS + FMT-control group, DSS + FMT-DSS group, and DSS + FMT-ACP group. The gut microbiota was first cleared by the antibiotic cocktail approach described above, and then received daily gavage administration of 200 μL of fresh bacterial solution for 14 days, with each group of mice receiving DSS to induce colitis on the latter 7 days.

2.3 Disease activity index (DAI) score

During DSS induction, the severity of colitis was assessed using the DAI score based on clinical symptoms of weight loss, fecal consistency, and bloody feces (Table S1). The DAI scale ranges from 0 to 4, with higher scores indicating more severe colitis.

2.4 Histopathological examination

Paraformaldehyde-fixed colon tissues were paraffin embedded and then sectioned (3 mm). After being dewaxed and rehydrated, the sections were stained with hematoxylin and eosin (H&E). Histopathological changes including inflammatory cell infiltration, mucosal injury, and depth of injury were evaluated. Detailed histologic scoring rules for colitis are shown in Table S2.

2.5 Protein extraction and Western blotting

The expression of the protein related to Occludin (1:1 000; Proteintech, Wuhan, China), zonula occludens 1 (ZO-1) (1:1 000; Proteintech, Wuhan, China), and mucin-2 (Muc2) (1:500; ABclonal, Guangzhou, China) were evaluated using Western blotting. Briefly, colonic segments were homogenized with RIPA buffer (Fudebio, Hangzhou, China) to extract proteins and quantified by BCA Protein Assay Kit (Thermo, MA, USA) according to the manufacturer's protocol. Protein samples were boiled for 15 min in protein loading buffer (Beyotime, Shanghai, China), electrophoresed on 10%–15% sodium dodecyl sulfate-polyacrylamide gelelectrophoresis (SDS-PAGE) and then transferred to PVDF membranes (Millipore Co., MA, USA). The PVDF membranes were blocked using 5% skimmed milk powder and then incubated with specific primary antibody at 4 °C overnight. The membranes were incubated with the HRP-labeled goat anti-mouse/rabbit IgG (Abmart, Shanghai, China) for 1 h, and then detected in darkroom using ECL kit (Fudebio, Hangzhou, China).

2.6 Immunofluorescence (IF) staining

IF staining was performed according to standard procedures. Colon tissue sections were dewaxed and hydrated, then high pressure boiled with Tris-EDTA (pH 9.0) or citrate buffer (pH 6.0) for antigen retrieval. After being blocked with 5% BSA for 1 h at 37 ℃, the sections were incubated overnight at 4 °C with the following primary antibodies: anti-Muc2 (1:200; Abcam, Cambridge, UK), anti-Occludin (1:200; CST, MA, USA), anti-ZO-1(1:1 000; Proteintech, Wuhan, China), anti-F4/80 (10 μg/mL; Thermo, MA, USA), and anti-CD206 (20 μg/mL; R&D Systems, MN, USA). The next day the sections were incubated with the appropriate fluorescent-labeled secondary antibody for 1 h at room temperature in the dark before staining the nuclei with DAPI (Beyotime, Shanghai, China). Finally, the images were observed under a fluorescence microscope (Olympus, Tokyo, Japan) and the mean fluorescence intensity of images was analyzed using ImageJ software (National Institutes of Health, MD, USA).

2.7 Alcian blue (AB) staining

Carnoy-fixed colon tissue fragments were stained using the AB Kit (Solarbio, Beijing, China) according to the protocol provided by the manufacturer.

2.8 Real-time quantitative PCR (RT-qPCR)

Total RNA was extracted using Trizol reagent (AG, Changsha, China), and then reverse transcription was performed using Reverse Transcriptase Kit (AG, Changsha, China) according to the manufacturer's protocol. RT-qPCR amplification was subsequently performed with SYBR Green Premix Ex Taq (Vazyme, Nanjing, China) using the Roche LC480 system. The mRNA expression was calculated using the $2^{-\Delta\Delta Ct}$ method with β-actin as the reference gene. Gene primer sequences are provided in Table S3.

2.9 Isolation of lamina propria mononuclear cells (LPMCs)

Colon tissue was dissected, cut longitudinally, rinsed in pre-cooled PBS (Gibco, CA, USA) to remove feces, and then cut into 1 cm intestinal segments. Colon fragments were incubated in D-Hanks Balanced Salt Solution (HBSS, calcium and magnesium free, Solarbio, Beijing, China) with 30 mmol/L $EDTANa_2$ (Solarbio, Beijing, China) and 2 mmol/L dithiothreitol (DTT) (Coolaber, Beijing, China) at 37 °C for 30 min on a constant temperature shaker. After filtration, the remaining colon tissues were continued to be incubated in HBSS (containing calcium and magnesium) with 0.2 mg/mL collagenase-D (Roche, Basilea, Switzerland), 0.05 mg/mL DNase I (Sigma, MO, USA), and 2 U/mL Dispase II (Coolaber, Beijing, China) at 37 °C for 30 min on a constant temperature shaker. The filtrate was collected through a 70 μm cell strainer, followed by density gradient centrifugation using 40%–80% Percoll (Solarbio, Beijing, China). The intermediate white membrane layer, corresponding to the enriched LPMCs, was then collected.

2.10 Flow cytometry

LPMCs were firstly incubated with anti-mouse CD16/32 (Biolegend, CA, USA) to block the Fc receptor, followed by incubation with APC labeled anti-F4/80, and Alexa Fluor® 700 labeled anti-CD206 (Biolegend, CA, USA) for 30 min at 4 °C for staining. The stained LPMCs were then examined by FACSCalibur flow cytometry instrument and the data were analyzed using FlowJo software version 10 (FlowJo, OR, USA).

2.11 16S rRNA gene sequencing

Fresh feces were collected from each group of mice to be used as 16S rRNA to detect the composition of the gut microbiota. Fecal genomic DNA was extracted with the E.Z.N.A.® Stool DNA Kit (Omega Bio-Tek, GA, USA) followed by PCR amplification using specific primers (341F and 806R) targeting the 16S rRNA V3-V4 region. The PCR products were purified using the AxyPrep DNA Gel Extraction Kit (Axygen Biosciences, CA, USA) and then tested by 2% agarose electrophoresis. Illumina sequencing libraries were constructed according to the instructions of the TruSeqTM DNA Sample Prep Kit (Illumina, CA, USA). The analysis was performed on the Illumina NovaSeq PE250 platform of Majorbio Bio-Pharm Technology Co. Ltd. (Shanghai, China).

2.12 Statistical analysis

SPSS 21.0 software (Version 21.0, IBM, NY, USA) was used for statistical analysis and GraphPad Prism 7 software (GraphPad Software, CA, USA) for graphical processing. All data were presented as mean ± standard deviation (SD) or mean ± standard error (SEM). Significant differences between groups were tested using one-way ANOVA and LSD multiple comparison test. $P < 0.05$ was considered statistically significant.

3. Results

3.1 Chemical structure of ACP

The primary structure of ACP was estimated in this study (Fig. 1). Comparing the peak retention time of the monosaccharide mixed standard with that of the ACP sample, ACP was mainly composed of glucose, galactose, and fucose, with a molar ratio of 11.4:1.9:1, and also contains a small amount of mannose and glucuronic acid (Figs. 1A and B). The Mw of polysaccharide is an important physicochemical parameter, which is closely related to the biological activity of polysaccharide[14]. Notably, polysaccharides with intestinal barrier protective effects have higher Mw, probably because high Mw polysaccharides can maintain the structural integrity of the intestinal barrier by forming something similar to the sticky gel[15-16]. Calculated with ASTRA6.1 software (Wyatt Technology, CA, USA), it was found that Mw of ACP was 2.7×10^6 Da, which is higher than that reported in previous studies, indicating that ACP might have the biological activity of protecting intestinal barrier. The characteristic chemical bond of ACP was further revealed by FT-IR spectroscopy. The spectrum showed a wide and strong O–H stretching vibration absorption peak at 3 432.51 cm^{-1}, which is the characteristic absorption peak of polysaccharides. The absorption peak at 2 923.95 cm^{-1} was assigned to C–H stretching vibration, and the absorption peak at 1 079.66 cm^{-1} was attributed to the C=O stretching vibrations of glucuronic acid (Fig. 1C). The molecular morphologies of ACP were observed using a scanning electronic microscope. As shown in Fig. 1D, ACP surface was rough and had porous structure. Rough surfaces and porous structure provide a larger surface area and more sites for interaction with other molecules[17], which may be the structural basis for ACP to exert its biological activity.

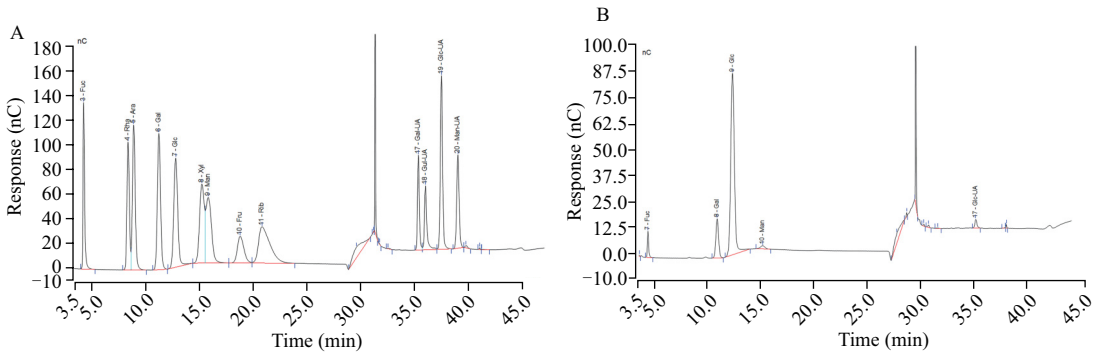

Fig. 1 Chemical structure of ACP. HPLC profiles of monosaccharide composition analysis of (A) mixed standards, (B) ACP. (C) Fourier transform infrared spectroscopy (FT-IR) analysis of ACP. (D) The scanning electron microscopy images (2 000×) of ACP.

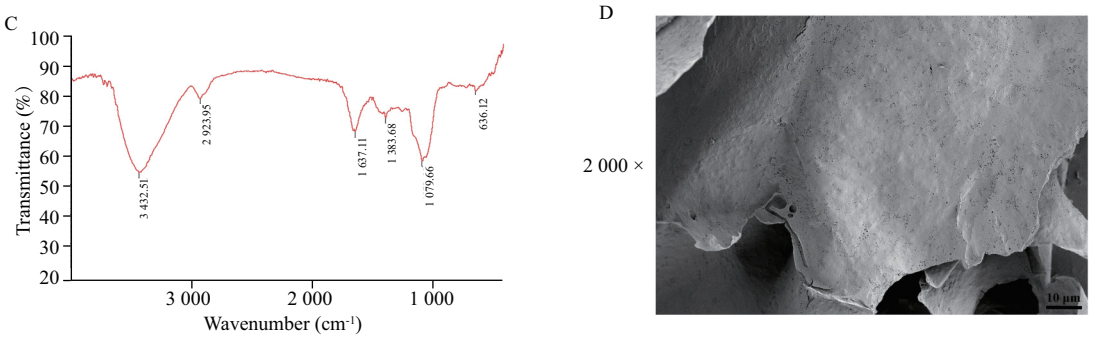

Fig. 1 (*Continued*)

3.2 ACP alleviated the symptoms of DSS-induced colitis in mice

The symptoms of DSS-induced colitis were evaluated by 3 parameters including body weight changes, DAI score and colon length. Compared with the control group, the DSS group showed significant decrease of body weight, increase of DAI score, and dramatic shortening of the colon, while high-ACP and low-ACP supplementation significantly reversed the tendency (Figs. 2B-E). Representative H&E staining histological sections and histopathology scores were shown in Fig. 2F. The colon tissues of the control group displayed a normal morphological structure with intact mucous membranes, and no inflammatory infiltration. In contrast, the colon tissues from the DSS group showed severe acute colitis, manifested by the destruction of the mucosal layer, disappearance of the crypt, marked edema of the submucosal and muscular, and extensive infiltration of inflammatory cells. Both the DSS + high-ACP and DSS + low-ACP groups alleviated these pathological damages and restored the integrity of the intestine. Additionally, there was a significant increase in histological scores following DSS treatment compared to those of the control group (Fig. 2G), while these changes were dramatically reversed by the supplementations of high-ACP and low-ACP. Collectively, these results revealed that ACP could effectively improve the symptoms of DSS-induced colitis in mice, and that high dose ACP is more effective than low dose ACP.

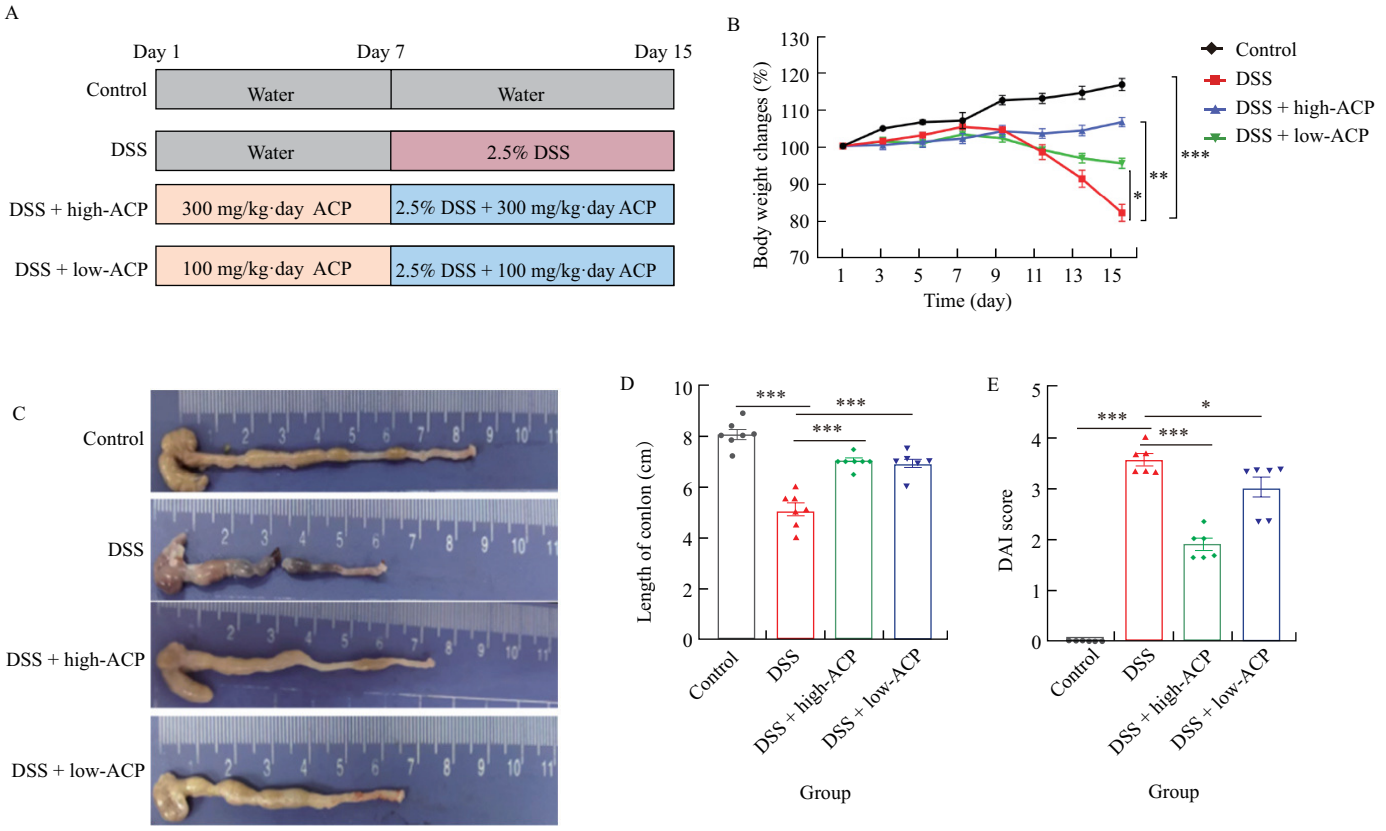

Fig. 2 ACP alleviated the symptoms of DSS-induced colitis in mice. (A) Diagram of the DSS-induced colitis mice model and ACP treatment protocol. (B) Body weight changes. (C) Photograph of the representative colons. (D) Length of colon. (E) DAI score. (F) Representative H&E staining images. Scale bar = 100 μm or 50 μm (downmost). (G) Histopathology score. The data were presented as the means ± SEM (n= 6). *P < 0.05; **P < 0.01; ***P < 0.001.

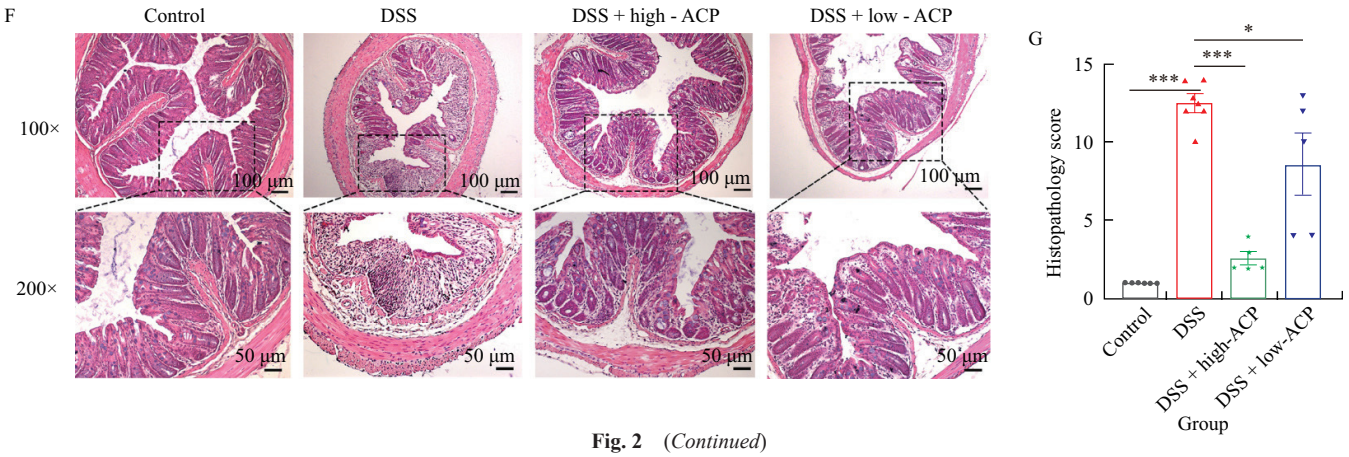

Fig. 2 (*Continued*)

3.3 ACP repaired intestinal mechanical barrier and mucus barrier in DSS-induced colitis

ZO-1 and Occludin are tight junction (TJ) proteins responsible for maintaining the mechanical barrier and permeability of the mucosal epithelium, and Muc2 is a high Mw glycoprotein secreted by goblet cells that plays an essential role in maintaining the mucus barrier of the mucosal epithelium. As shown in Fig. 3A, the protein expression levels of ZO-1, Occludin and Muc2 were significantly decreased in DSS group compared with the control group, whereas ACP intervention significantly up-regulated ZO-1, Occludin and Muc2 expression in DSS + low-ACP group and DSS + high-ACP group ($P < 0.05$, Fig. 3A). Consistent with the Western blotting results, the IF results likewise indicated that the protein levels of Muc2, ZO-1 and Occludin were significantly increased after ACP intervention ($P < 0.05$, Figs. 3C and D). Similarly, the same results were found at the transcriptional level by RT-qPCR assay (Fig. 3B). In addition, with the AB results in Fig. 3E, we again revealed the repairing effect of ACP on the intestinal mucus barrier in DSS colitis. The above results demonstrated that ACP can alleviate DSS-induced dysfunction of intestinal mechanical barrier and mucus barrier.

3.4 ACP promoted M2 macrophage polarization and suppressed intestinal inflammation in colitis mice

The lamina propria of the colon serves as the primary effector site of the mucosal immune response, and macrophages are the most abundant immune cells residing in the lamina propria. Macrophages are highly plastic, which can be activated by changes in the surrounding local microenvironment, cytokines and metabolites, and differentiate into different subtypes and obtain different functional phenotypes[18]. Decreased M2 macrophages in the lamina propria of the colon have been found in IBD patients, and M2 macrophages have been shown to relieve intestinal inflammation and promote tissue repair[19]. Therefore, we examined the proportion of M2 macrophages in the colon lamina propria cells of mice in each group. Flow cytometry results showed a significant decrease in the proportion of M2 macrophages in the DSS group compared to the control group, whereas M2 macrophages in the lamina propria increased significantly after ACP administration (Figs. 4A and B). Meanwhile, IF of mouse colon tissues was validated and it was also found that ACP increased the proportion of M2 macrophages, that is, promoted the M2 macrophages polarization (Fig. 4C). Additionally, the mRNA levels of M2 macrophage markers (Arg1 and CD206) in the DSS + high-ACP and the DSS + low-ACP groups were significantly increased compared to the DSS group (Fig. 4D). Moreover, ACP could reduce the elevated expression of IL-1β, IL-6, and TNF-α and up-regulate the reduced expression of IL-10 in DSS-induced colitis mice at the mRNA level (Fig. 4E). These above data indicated that ACP could promote M2 macrophages polarization and relieve intestinal inflammation, and thus restore the intestinal immune barrier homeostasis in colitis.

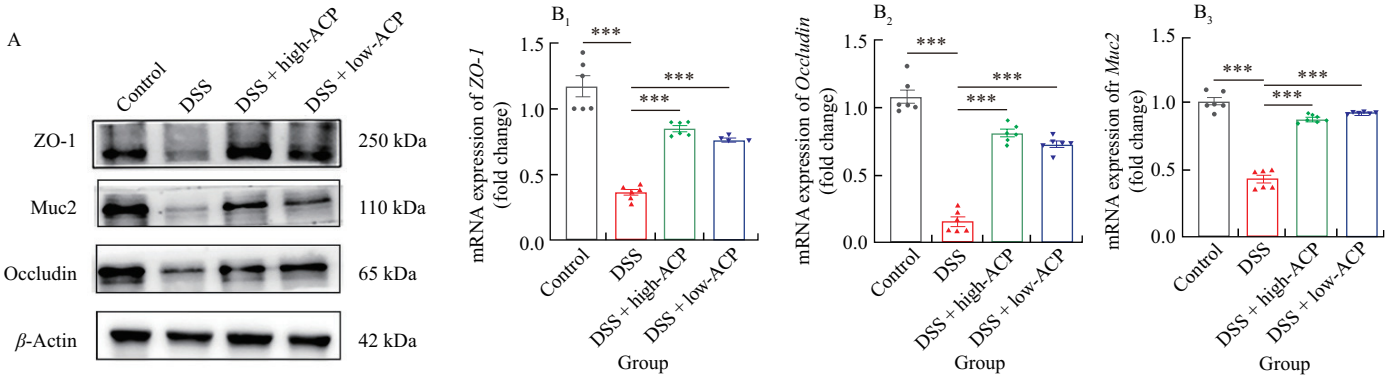

Fig. 3 ACP repaired intestinal barrier function in DSS-induced colitis. (A) Expression of barrier-associated proteins (ZO-1, Muc2, Occludin) were measured by Western blotting. (B) The relative mRNA level of *ZO-1*, *Occludin* and *Muc2* was detected by RT-qPCR. (C) Representative images of IF staining of ZO-1, Occludin and Muc2. Scale bar = 50 μm. (D) Mean fluorescence intensity of ZO-1, Occludin and Muc2. (E) AB staining of each group. Scale bar = 50 μm. All data were presented as the means ± SEM ($n = 6$). ***$P < 0.001$.

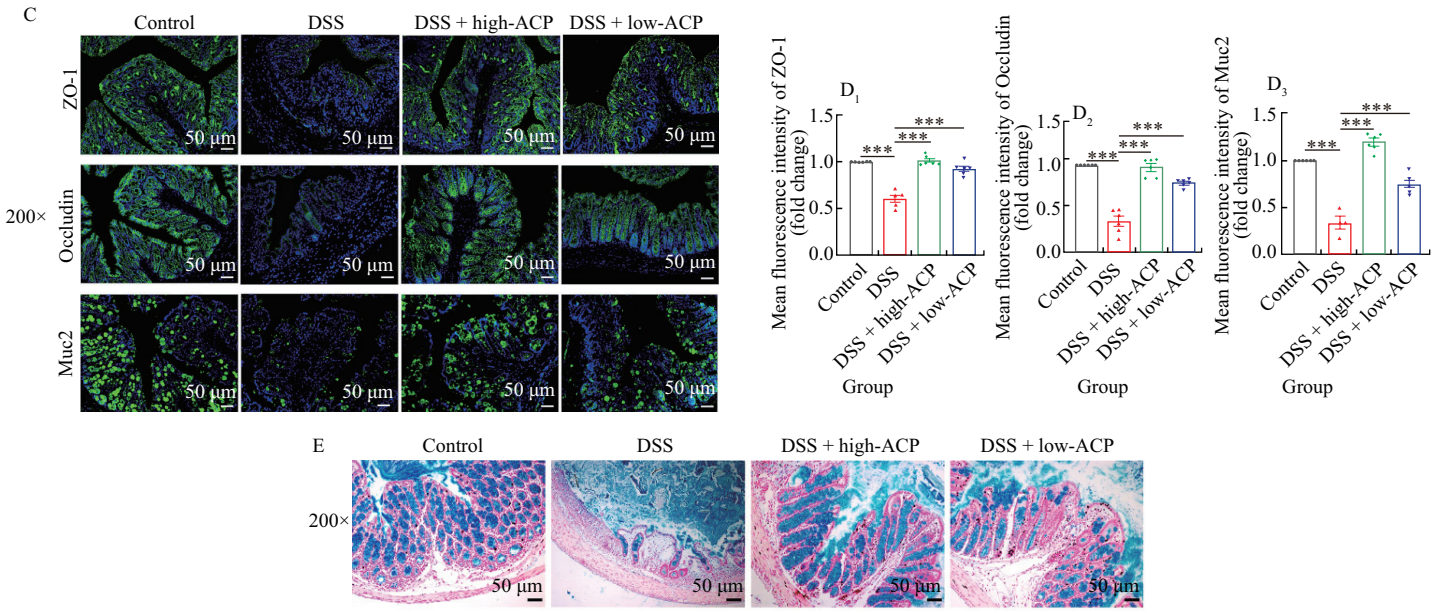

Fig. 3 (*Continued*)

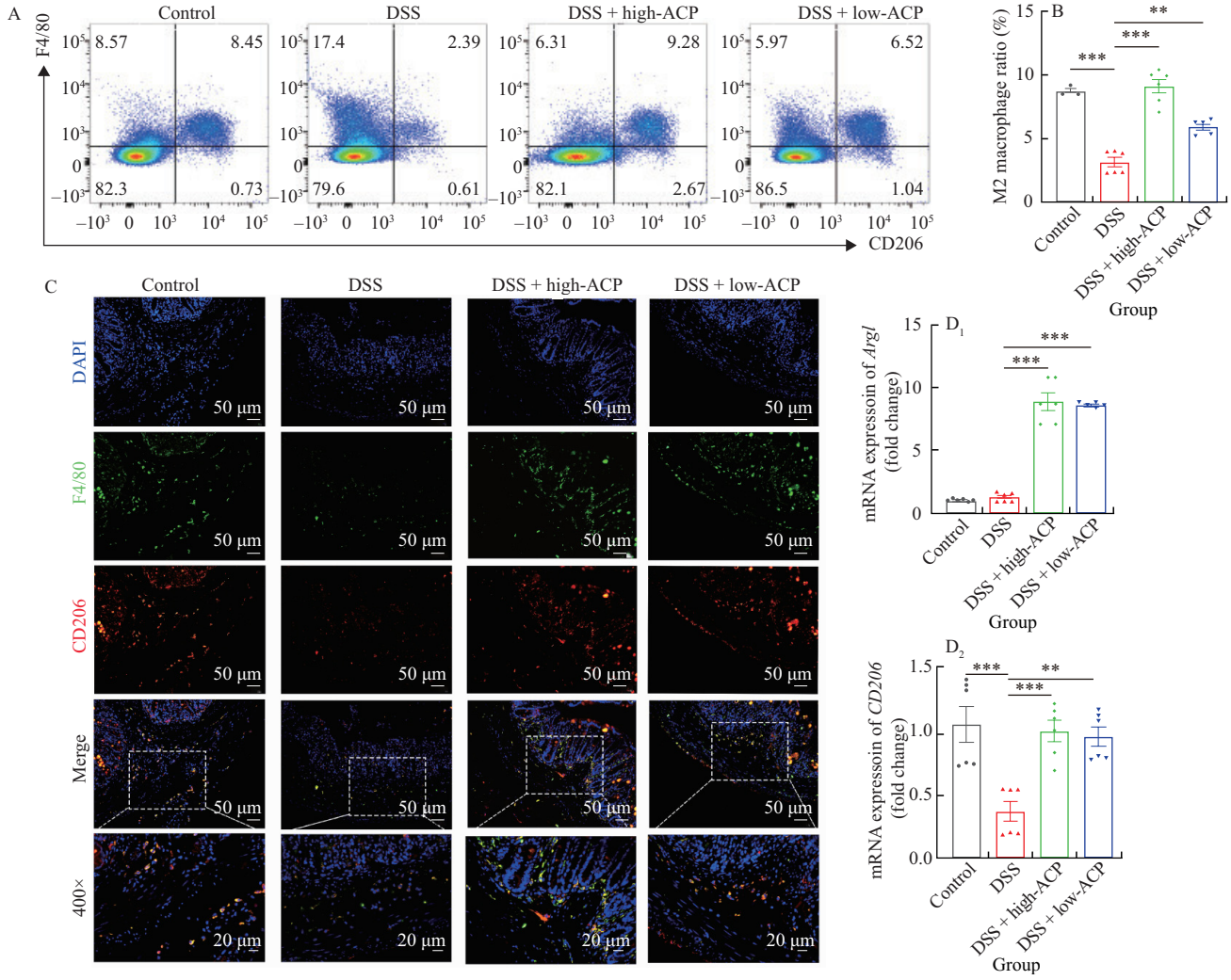

Fig. 4 ACP promoted M2 macrophage polarization and suppressed intestinal inflammation in colitis mice. (A) LPMCs were isolated, stained for F4/80 (macrophage markers) and CD206 (M2 macrophage markers), and determined by flow cytometry. (B) The ratio of M2 macrophage was detected by flow cytometry. (C) Representative IF staining of F4/80 (green) and CD206 (red). Nuclear counterstaining was provided with DAPI (blue). Scale bar = 50 μm or 20 μm (downmost). (D) The relative mRNA level of M2 macrophage markers (*Arg1* and *CD206*). (E) The relative mRNA level of *IL-1β*, *IL-6*, *TNF-α* and *IL-10*. All data were presented as the means ± SEM ($n = 6$). $^{**}P < 0.01$; $^{***}P < 0.001$.

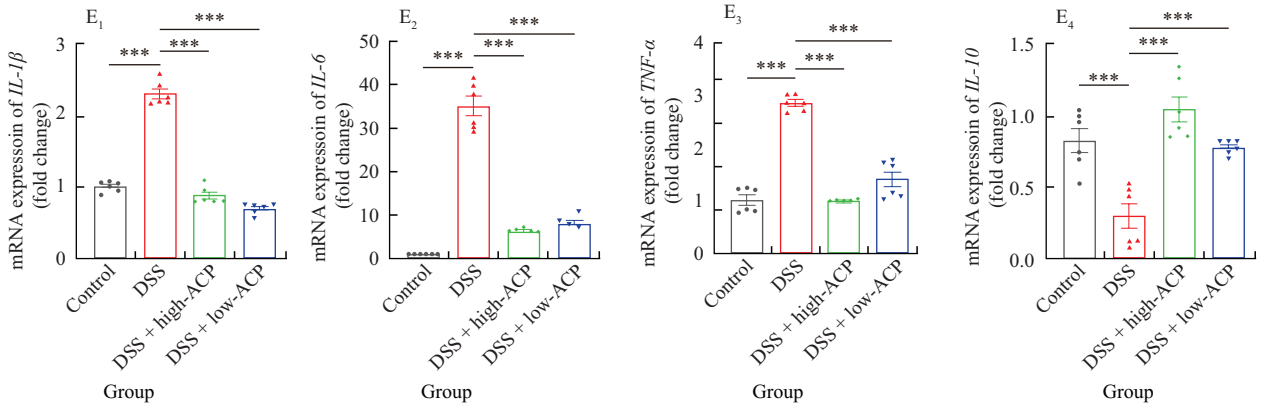

Fig. 4 (*Continued*)

3.5 *ACP attenuated DSS-induced gut microbiota dysbiosis*

Gut microbiota plays an important role in maintaining intestinal biological barrier homeostasis, and intestinal dysbiosis is a key pathogenetic factor of IBD[20]. To evaluate the effect of ACP on the gut microbiota in colitis mice, 16S rRNA amplicon sequencing was performed. As shown in Figs. 5A and B, a decrease in the gut bacterial alpha diversity, measured with Shannon index and Sobs index, was observed in the DSS group. In contrast, the ACP intervention significantly limited the loss of α-diversity in the DSS + high-ACP and DSS + low-ACP groups, indicating a protective effect of ACP on gut microbiota. β-Diversity analysis with principal component analysis (PCoA) and NMDS analysis (Figs. 5C and D) showed that the gut microbiota composition in the DSS group was significantly different from that of the control group. And ACP intervention reversed the DSS-induced changes in gut microbiota, suggesting that ACP can significantly affect the gut microbiota structure in colitis mice. Compositionally, the dominant phyla were Firmicutes, Bacteroidota, Verrucomicrobia, Desulfobacterota, and Proteobacteria for all the 4 groups (Fig. 5E). The Firmicutes/Bacteroidetes (F/B) ratio was found to be decreased in the DSS group compared with the control group, while the ACP treatment group could effectively reverse this change (Fig. 5F).

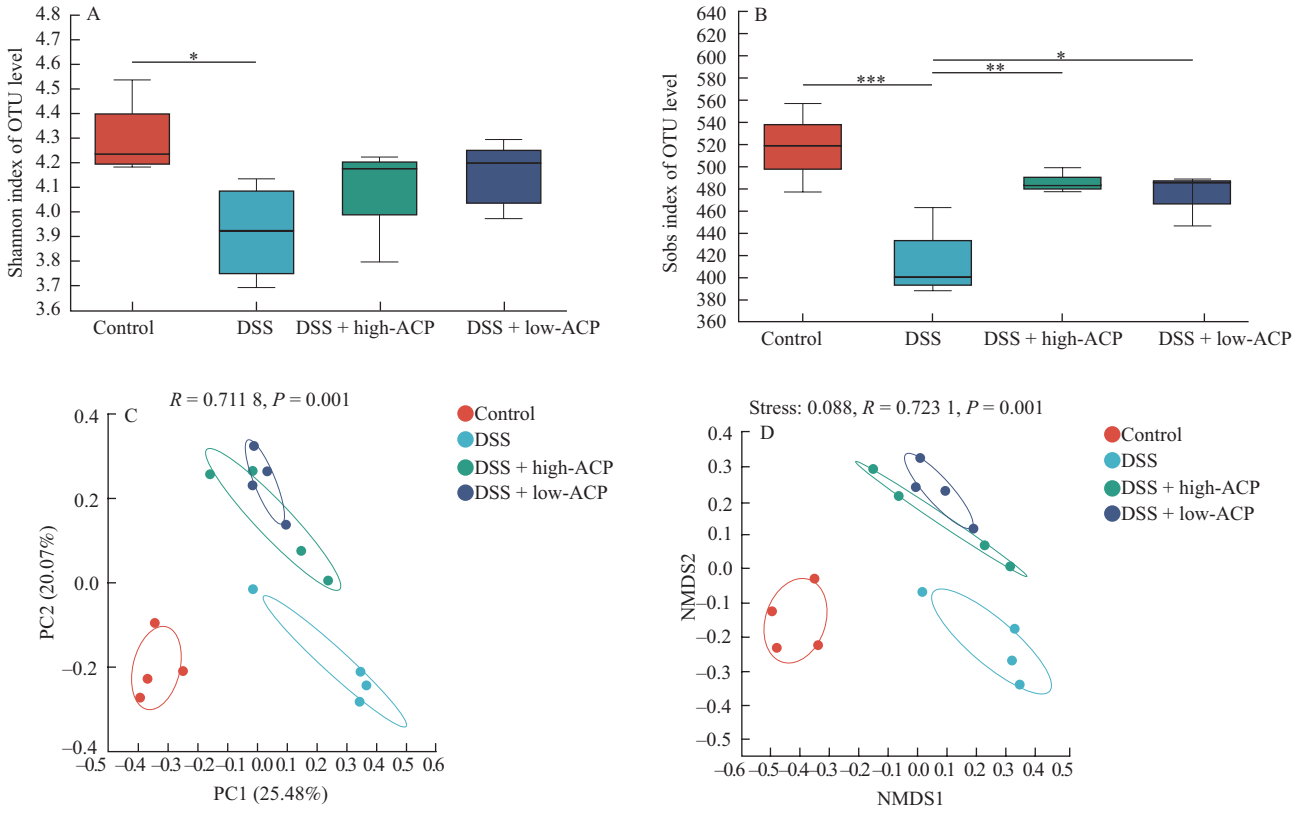

Fig. 5 ACP attenuated DSS-induced gut microbiota dysbiosis. (A) Shannon index of OTU level. (B) Sobs index of OTU level. (C) The principal coordinate analysis (PCoA) on OTU level. (D) NMDS analysis on OTU level. (E) The percent of community abundance on phylum level. (F) F/B ratio. (G) Comparison of different microbiota between the control group and DSS group on genus level. (H) Comparison of different microbiota between the DSS group and DSS + high-ACP group on genus level. *$P < 0.05$; **$P < 0.01$; ***$P < 0.001$; ns, not significant.

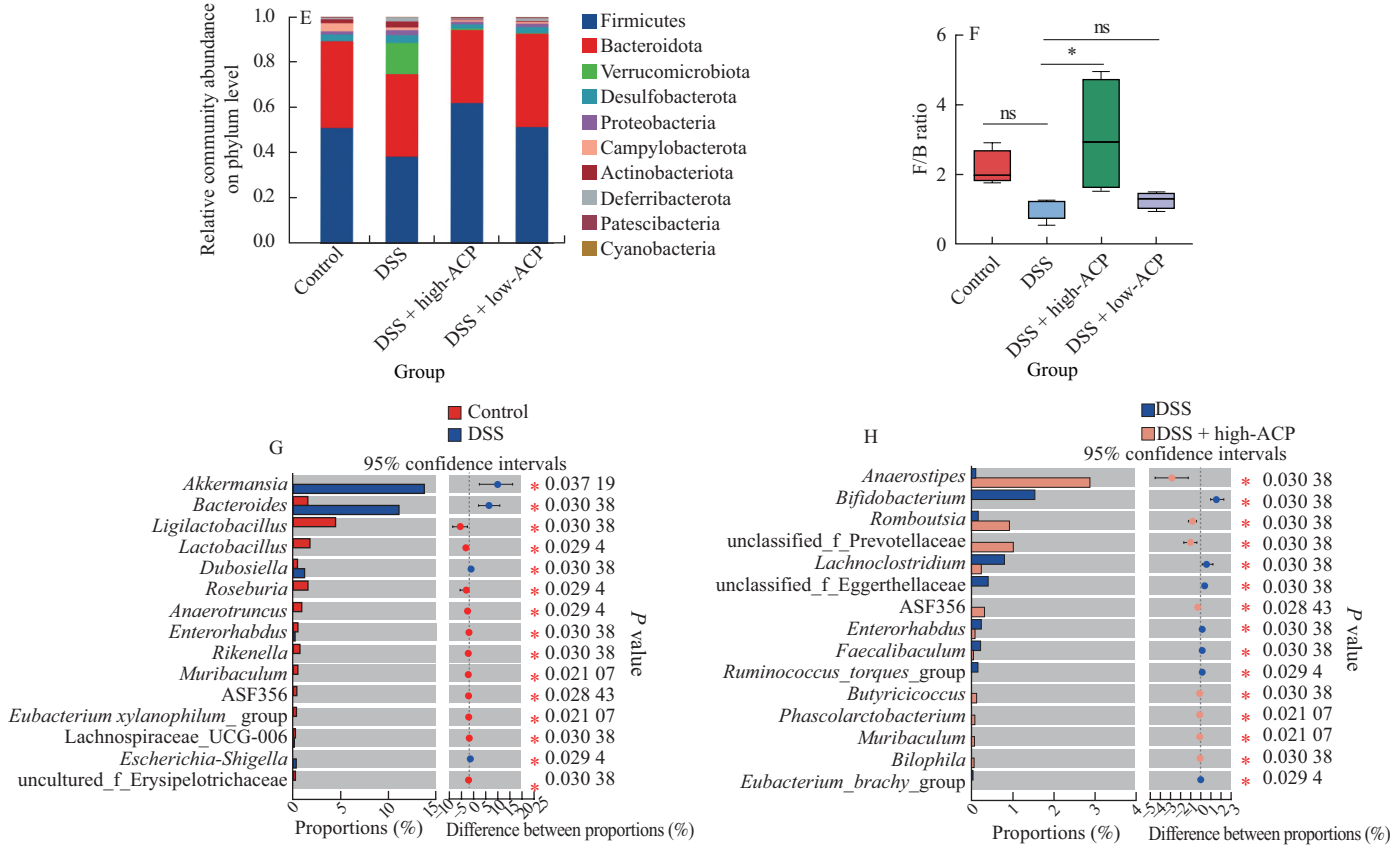

Fig. 5 (*Continued*)

The above results indicated that the effect of ACP on improving intestinal barrier and reducing intestinal inflammation was in a dose-dependent manner. The differences in the gut microbiota among the control, DSS, and DSS + high-ACP groups were further accessed at the genus level using the Wilcoxon rank sum test (Figs. 5G and H). Compared with the control group, the relative abundance of *Akkermansia*, *Bacteroides*, *Dubosiella* and *Escherichia-Shigella* induced by DSS treatment increased significantly, while the relative abundance of *Ligilactobacillus*, *Lactobacillus*, *Roseburia*, *Anaerotruncus*, *ASF356* and *Enterorhabdus* decreased significantly. However, high-ACP treatment significantly increased the relative abundance of *Anaerostipes*, *Romboutsia*, *Butyricoccus*, *ASF356*, *Phascolarctobacterium*, and unclassified_f_Prevotellaceae, which suggested that ACP could reverse the microflora disturbance of DSS colitis.

3.6 *Effect of ACP on alleviating colitis depended on the gut microbiota*

To determine the significance of gut microbiota in the protective effect of ACP against colitis, we cleared the gut microbiota of mice before DSS administration. Mice were given antibiotics (ABX) cocktail for 14 days to clear the gut microbiota and then modeled with drinking water containing 2.5% DSS (Fig. 6A). There were no statistically significant differences between the DAI scores, body weight changes, colon length, and pathological histology exhibited in the ABX + DSS group and the ABX + DSS + ACP group (Figs. 6B-E). Moreover, the function of ACP to repair the intestinal mechanical and mucus barriers was decreased after removing the gut microbiota (Figs. 6F-G). These results suggested that the protective effect of ACP against DSS-induced colitis relied on gut microbiota.

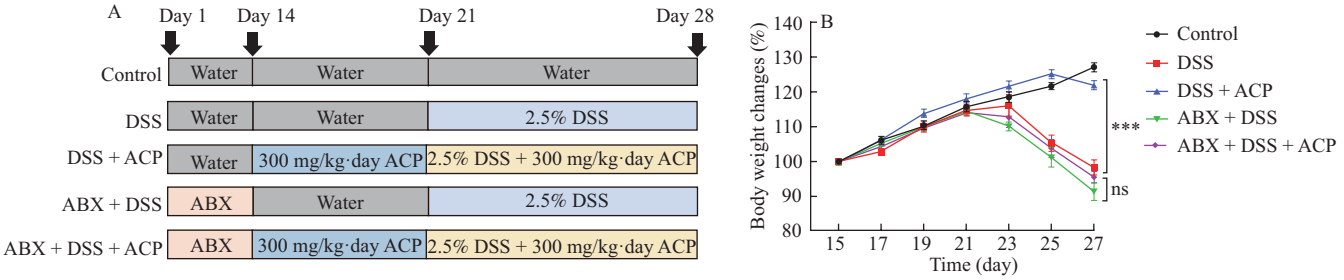

Fig. 6 Effect of ACP on alleviating colitis depended on the gut microbiota. (A) Diagram of the antibiotic cocktail protocol. (B) Body weight changes. (C) DAI score. (D) Colon length. (E) Representative H&E staining images. Scale bar = 100 μm or 50 μm (downmost). (F) Representative images of IF staining of ZO-1, Occludin and Muc2. Scale bar = 50 μm. (G) AB staining of each group. Scale bar = 50 μm. All data were presented as the means ± SEM (n = 6). ***P < 0.001; ns, not significant.

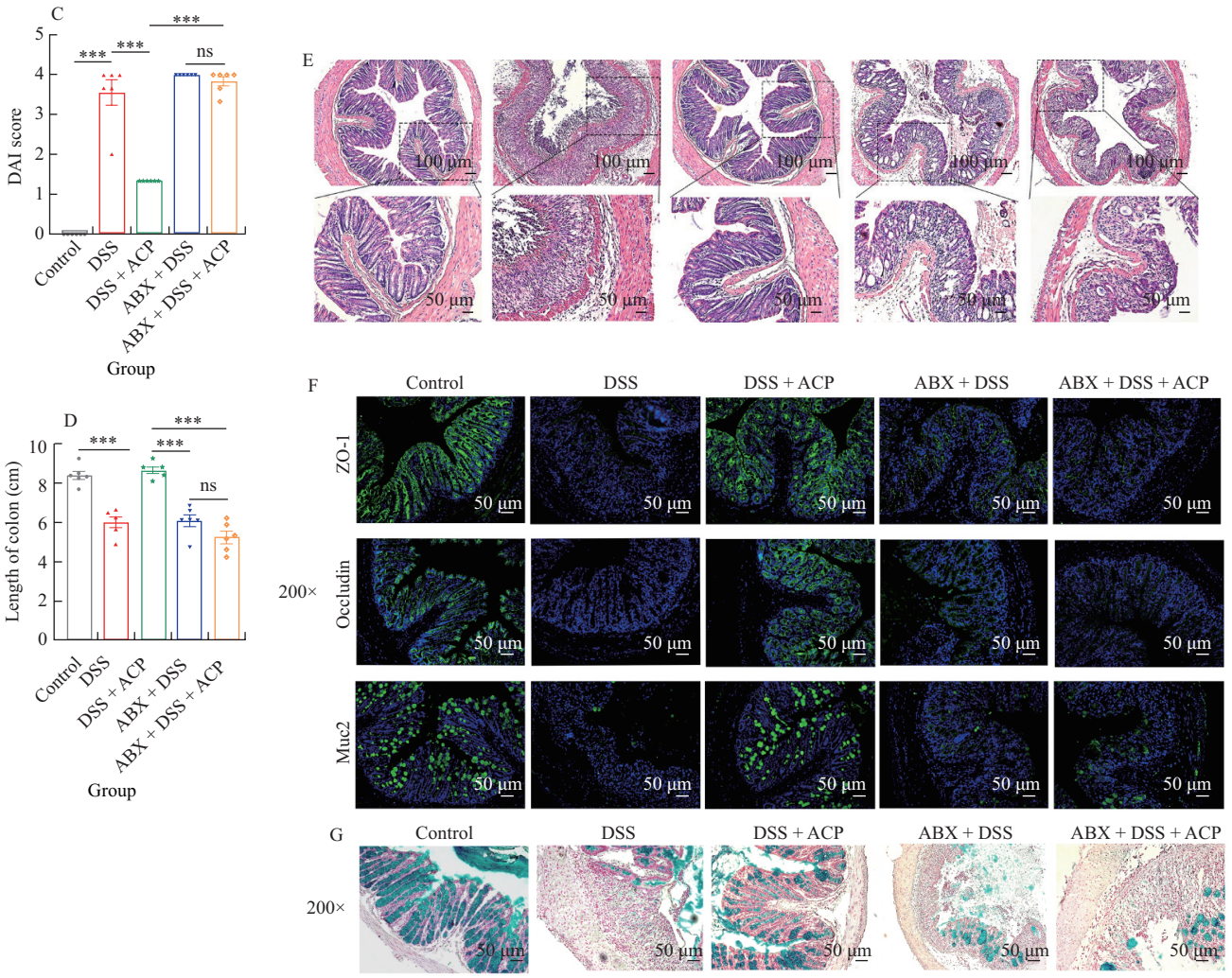

Fig. 6 (*Continued*)

3.7 Fecal microbiota of ACP-treated mice restored intestinal damage in DSS-induced colitis

To further determine the role of gut microbiota in the treatment of colitis with ACP, we transplanted fecal suspensions from donor mice into the corresponding recipient mice (Fig. 7A). As shown in Fig. 7C, the DAI scores in the DSS + FMT-ACP group were significantly decreased compared with those in the DSS + FMT-DSS group. Likewise, DSS + FMT-ACP treatment significantly improved weight loss and colon shortening in mice with DSS injury (Figs. 7B and D). Histopathologic results showed that colonic epithelial cell destruction, inflammatory cell infiltration, and crypt disappearance were significantly improved in the DSS + FMT-ACP group compared with the DSS + FMT-DSS group (Fig. 7E). The intestinal barrier damage was further investigated in colitis mice with FMT. Compared with the DSS + FMT-DSS group, the expression of ZO-1, Occludin and Muc2 in DSS + FMT-ACP group was significantly increased (Fig. 7F). Similarly, the AB results suggested that the DSS + FMT-ACP group could promote colonic mucin secretion and repair the mucus barrier (Fig. 7G). The above results demonstrated that the protective effect of ACP against DSS colitis was dependent on gut microbiota.

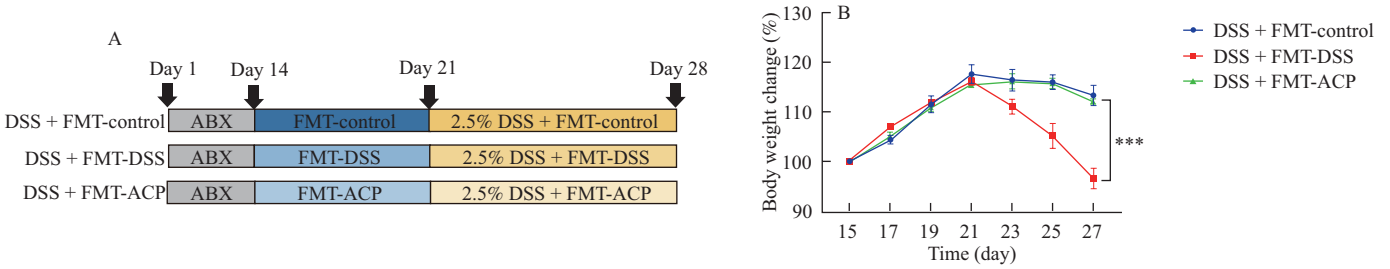

Fig. 7 Fecal microbiota of ACP-treated mice restored intestinal damage in DSS-induced colitis. (A) Diagram of the FMT protocol. (B) Body weight changes. (C) DAI score. (D) Length of colon. (E) Representative H&E staining images. Scale bar = 100 μm or 50 μm (downmost). (F) Representative images of IF staining of ZO-1, Occludin and Muc2. Scale bar = 50 μm. (G) AB staining of each group. Scale bar = 50 μm. All data were presented as the means ± SEM (n = 6). $^{**}P < 0.01$; $^{***}P < 0.001$.

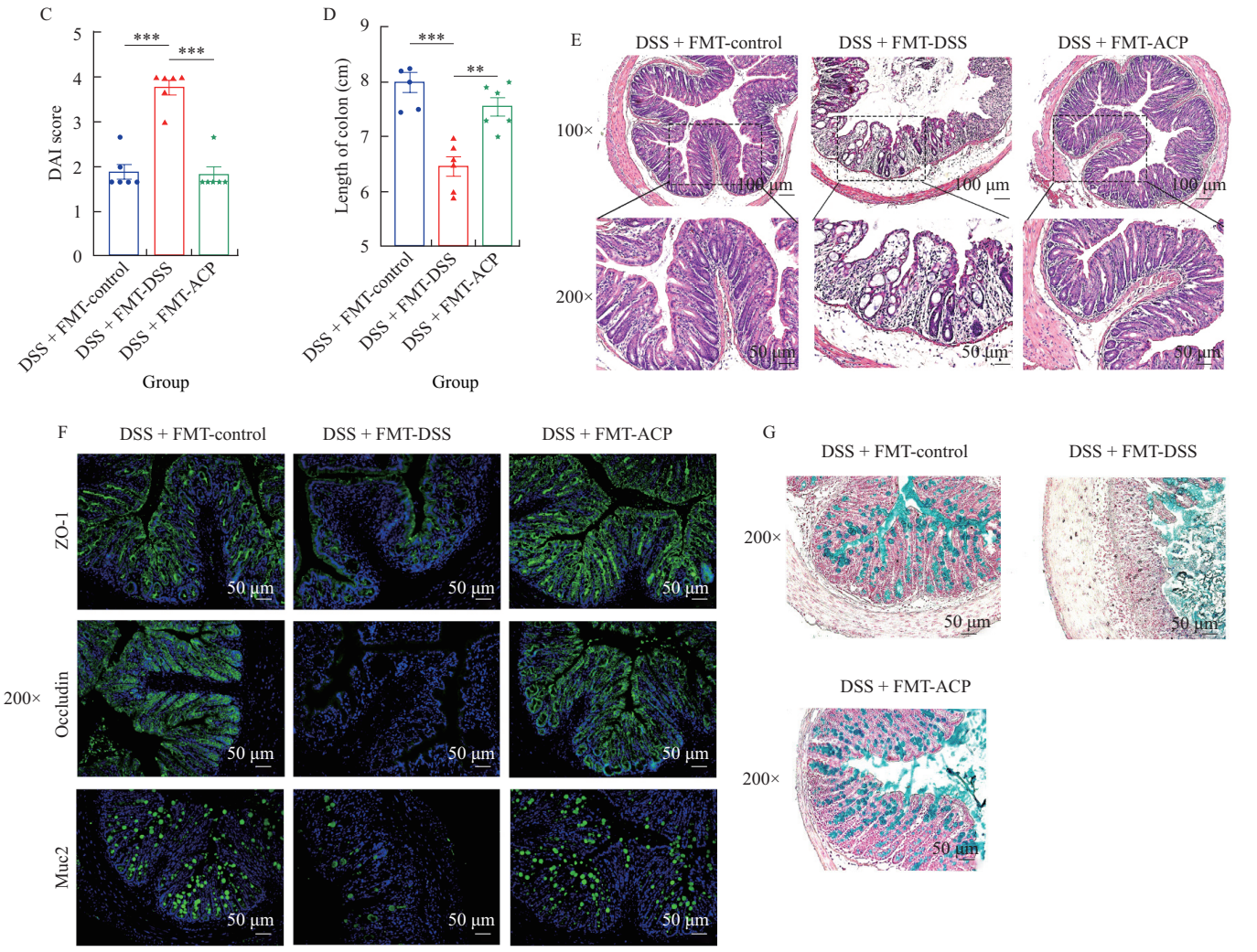

Fig. 7 (*Continued*)

3.8 Regulation of M2 macrophage polarization by ACP depended on the gut microbiota

According to previous results, ACP administration not only modulated the gut microbiota, but also modulated intestinal M2 macrophage polarization. Here we further explored the role of the gut microbiota on macrophage polarization during intestinal inflammation. Flow cytometry results showed that after elimination of gut microbiota, ACP lost its effect on regulating intestinal M2 macrophage polarization in DSS colitis mice (Figs. 8A and B). After FMT, the proportion of M2 macrophages in the colon was significantly restored in the DSS + FMT-ACP group (Figs. 8C and D). These results were likewise confirmed by IF staining of the colon tissue (Figs. 8E and F). Taken together, these data suggested that the modulatory effect of ACP on M2 macrophage polarization during intestinal inflammation was exerted through the gut microbiota.

4. Discussion

Dietary component interventions have been reported to have great potential in alleviating IBD by modulating intestinal mucosal immunity and regulating gut microbiota[7,21], especially the polysaccharide[9,22]. ACP has been demonstrated to possess a wide range of biological activities such as antioxidant, anti-aging, anti-obesity and anticancer, with no adverse effects after consumption[23-25]. However, the role of ACP in DSS colitis has not been studied. In this study, the mice showed significant weight loss, severe hematochezia and diarrhea in colitis, while ACP treatment increased body weight, colon length, and decreased DAI score, as well as alleviated colon pathological damage, restored crypt structure, and reduced inflammatory cell infiltration. The alleviative effect of ACP on DSS-induced colitis was demonstrated, suggesting that ACP may be an effectively functional food supplement to mitigate IBD.

Intestinal mucosal barrier dysfunction is the main pathogenesis of IBD[26-27]. TJ is an important structural basis for maintaining the mechanical barrier between intestinal mucosal epithelial cells. Intestinal epithelial cells are tightly coupled *via* TJ proteins (e.g., ZO-1 and Occludin), which further prevents the invasion of pathogens, and thus maintains the structural and functional integrity of the intestinal barrier[28]. The mucus layer on the intestinal surface consists mainly of mucins (Muc2) secreted by intestinal goblet cells, forming a protective layer that protects the intestinal epithelium from

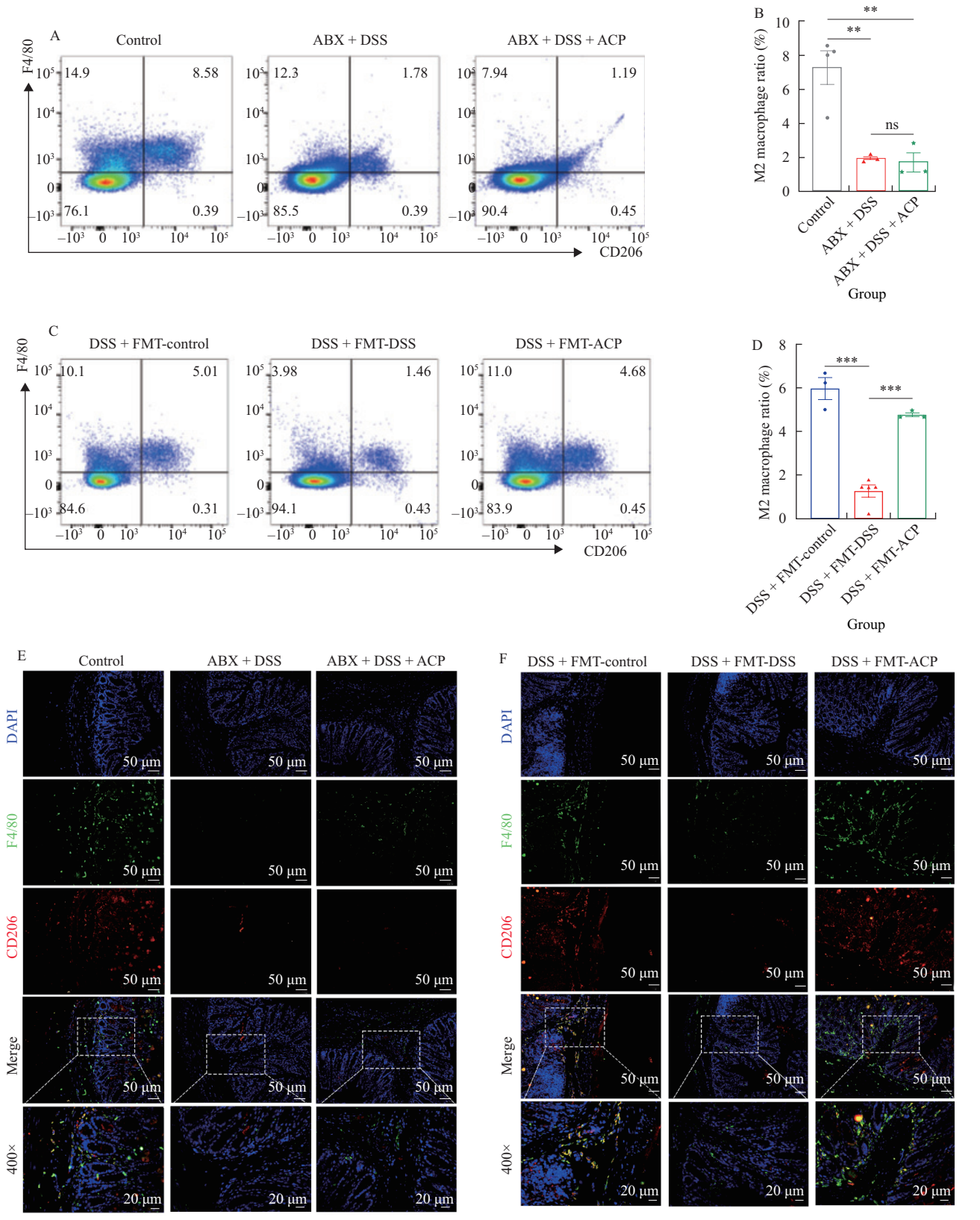

Fig. 8 Regulation of macrophages by ACP depended on the gut microbiota. Flow cytometry analysis of M2 macrophage marker CD206 expression and bar graphs show the relative mean ratio of CD206+ cells in F4/80+ population after (A, B) ABX and (C, D) FMT. Representative IF staining of F4/80 (green) and CD206 (red) after (E) ABX and (F) FMT. Scale bar = 50 μm or 20 μm (downmost). All data were presented as the means ± SEM. $^{**}P < 0.01$; $^{***}P < 0.001$; ns, not significant.

physical, chemical and microbial damage[29]. Thus, mucins and TJ proteins synergistically promote intestinal epithelial homeostasis. The loss of barrier integrity increases bacterial antigen translocation and stimulates intestinal mucosal inflammation, which is a core pathological feature of IBD[30]. Therefore, maintaining the integrity of the intestinal barrier is also an important goal of IBD treatment. In our study, we found that the expression of TJ proteins and Muc2 were significantly reduced in DSS colitis mice, suggesting that the intestinal mucosal barrier was impaired. After ACP treatment, the expression of ZO-1, Occludin, and Muc2 proteins significantly up-regulated, indicating that ACP repaired the mechanical and mucus barriers in DSS colitis mice and maintained the integrity of the intestinal mucosal barrier. The restoration and maintenance of intestinal mucosal barrier helps to improve the defense function of intestinal mucosa, thus promoting the remission of colitis.

As the key gatekeepers of intestinal innate immunity, macrophages play an essential role in maintaining intestinal immune homeostasis as they monitor the intestinal environment and phagocytose potentially harmful antigens[31]. It has been reported that macrophages can polarize from M0 to multiple phenotypes, with M1 and M2 phenotype playing key roles in IBD development and mucosal repair, respectively[32-33]. This suggests that the state of macrophage polarization may be a key factor in determining the resolution or progression of inflammation[19]. M2 macrophages are an anti-inflammatory phenotype involved in tissue repair and maintenance of intestinal homeostasis. As well, a large number of current studies suggested that transforming macrophages into anti-inflammatory M2 phenotypes is a promising therapeutic strategy for IBD[34-35]. In the present study, ACP significantly increased the proportion of M2 macrophages, indicating that ACP could promote M2 macrophage polarization in colitis mice. It may be the key factor for ACP to relieve intestinal inflammation by regulating intestinal immune barrier.

Dysbiosis of the gut microbiota is recognized as a trigger for IBD-initiating events[4,20]. The researchers observed changes in the composition of the gut microbiota in the IBD patient population, mainly manifested by decreased levels of beneficial bacteria and increased relative abundance of harmful bacteria[36-37]. The imbalance of microbial homeostasis leads to the colonization and invasion of opportunistic pathogens in the gut, which increases the risk of host immune responses and damages the intestinal biological barrier, thereby promoting the development of IBD. Here, we investigated the effects of ACP on the gut microbiota of DSS-induced colitis mice. The results showed that the diversity and richness of gut microbiota in mice with colitis were increased after ACP supplementation, and the β-diversity analysis also suggested that ACP could significantly affect the structure of intestinal microflora in colitis mice. Firmicutes and Bacteroidetes are the 2 most important bacterial phyla in the gastrointestinal tract, and the F/B ratio is widely regarded as a biomarker of gut dysbiosis[38]. Decreased F/B ratio have been found in patients with IBD[39], which may be associated with an immune-inflammatory response induced by decreased production of short-chain fatty acids (SCFAs), protein metabolite histamine, and lipopolysaccharide accumulation. It was found that the F/B ratio was decreased in the DSS group compared to the control group, while the ACP-treated group could effectively restore the decrease of the F/B ratio, which is important for maintaining the host intestinal homeostasis. It has been reported that intestinal commensal *Anaerostipes* can convert inositol into propionate and acetate, which demonstrates the potential benefits of *Anaerostipes* in maintaining intestinal homeostasis and promoting host health[40]. *Romboutsia*[41], *Butyricicoccus*[42], and *Phascolarctobacterium*[43] have also been proved to be SCFAs-producing bacteria, which decompose carbohydrates into SCFAs, thereby providing an energy source for intestinal epithelial cells, regulating intestinal microecological environment, and reducing intestinal inflammation. Therefore, it can be concluded that ACP increased the abundance of SCFAs-producing bacteria (*Anaerostipes*, *Romboutsia*, *Butyricicoccus* and *Phascolarctobacterium*) and maintained a dynamic balance of favorable intestinal microbiota, thus suppressing intestinal inflammation. To further elucidate the modulatory effects of ACP on the intestinal microbiota of DSS-induced colitis, we conducted ABX and FMT experiments. The results showed that after clearing the intestinal flora, ACP lost its protective effect against DSS colitis mice, and this protective effect could be transferred by FMT. The above results further suggested that the protective effect of ACP against DSS colitis was dependent on the intestinal microbiota.

Notably, the relationships among gut microbiota, immune response, and intestinal mucosal barrier in IBD have been increasingly reported[44-45]. The gut microbiota has been reported to modulate intestinal immunity, with the commensal microbiome regulating the maturation of the mucosal immune system, while the pathogenic microbiome contributes to immune dysfunction and lead to disease progression[6,44]. The changes in the gut microbiota affect the polarization state of macrophages, thus disrupting the balance of intestinal immunity. In our research, it was demonstrated that ACP increased the abundance of SCFAs-producing bacteria. Previous studies have reported that metabolites produced by gut microbes, particularly SCFAs, can promote M2 macrophage polarization[46-47]. SCFAs not only provide energy to the intestinal epithelial cells, but also induce the production of anti-inflammatory cytokines by binding to G-protein-coupled receptors (e.g., GPR43) on the surface of macrophages[48]. In addition, SCFAs can also enhance the M2 macrophage phenotype by inhibiting histone deacetylases (HDACs)[49]. Based on these findings, we hypothesized that ACP promotes macrophage polarization by enhancing the presence of SCFA-producing bacteria. To verify whether the regulation of macrophages by ACP was dependent on gut microbiota, we further examined macrophage changes after ABX and FMT. It was found that after ABX, ACP lost its regulatory effect on M2 macrophage polarization, whereas it was able to restore its regulatory effect on macrophages after FMT. In essence, ACP exhibits the potential to modulate the composition of the gut microbiota, fostering the growth of beneficial bacteria, which in turn promotes the polarization of colonic M2 macrophages and facilitates the repair of the intestinal mucosal barrier in DSS-induced colitis (Fig. 9). This study also has its limitations. Firstly, the precise chemical structure of ACP requires further elucidation. Secondly, the specific mechanisms by which ACP influences macrophage polarization through the gut microbiota warrant further investigation.

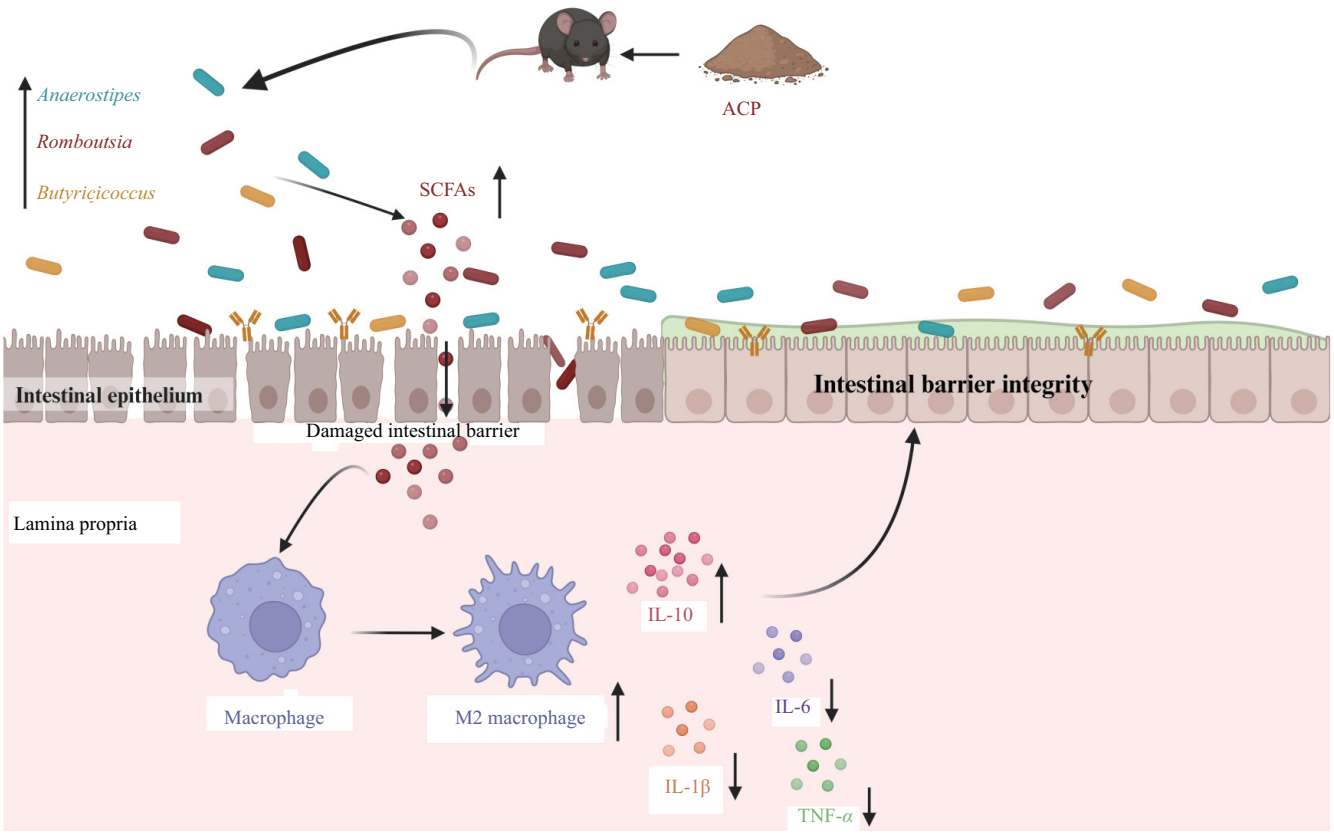

Fig. 9 Possible mechanism of ACP regulating DSS-induced colitis. ACP may regulate the structure and composition of the intestinal microbiota and promote the growth of beneficial bacteria such as SCFAs-producing bacteria (*Anaerostipes*, *Romboutsia*, and *Butyricicoccus*), which in turn promote the intestinal M2 macrophage polarization, further repair the intestinal mucosal barrier in DSS-induced colitis.

5. Conclusion

Our study demonstrated that ACP treatment can effectively attenuate gut microbiota dysbiosis and intestinal mucosal barrier damage in DSS-induced colitis mice. Further analysis showed that ACP may regulate the structure and composition of the intestinal microbiota and promote the growth of beneficial bacteria such as SCFAs-producing bacteria, which in turn promote the intestinal M2 macrophage polarization, further repair the intestinal mucosal barrier in DSS-induced colitis. These findings suggested that ACP can be used as a functional food ingredient for maintaining intestinal immune homeostasis, regulating intestinal microbiota and repairing the intestinal mucosal barrier, and are promising for application in dietary interventions for IBD treatment.

Declaration of interests

The authors declare that they have no known competing financial interests or personal relationships that could have appeared to influence the work reported in this paper.

Acknowledgement

This work was supported by National Natural Science Foundation of China (82070543, 82270581), National Key R&D Program of China (2021YFA0717001) and Shenzhen Science and Technology Program (KCXFZ20211020163558024). The authors also acknowledge the valuable contribution of biorender.com in creating the mechanism diagram for this study.

Appendix A. Supplementary data

Supplementary data associated with this article can be found, in the online version, at http://doi.org/10.26599/FSHW.2024.9250440.

References

[1] J.T. Chang, Pathophysiology of inflammatory bowel diseases, N. Engl. J. Med. 383 (2020) 2652-2664. https://doi.org/10.1056/NEJMra2002697.
[2] G.G. Kaplan, The global burden of IBD: from 2015 to 2025, Nat. Rev. Gastroenterol. Hepatol. 12 (2015) 720-727. https://doi.org/10.1038/nrgastro.2015.150.
[3] Z.B. Cai, S. Wang, J.N. Li, Treatment of inflammatory bowel disease: a comprehensive review, Front. Med. (Lausanne) 8 (2021) 765474. https://doi.org/10.3389/fmed.2021.765474.
[4] Y. Haneishi, Y. Furuya, M. Hasegawa, et al., Inflammatory bowel diseases and gut microbiota, Int. J. Mol. Sci. 24 (2023) 3817. https://doi.org/10.3390/ijms24043817.
[5] M.R. Spalinger, A. Sayoc-Becerra, A.N. Santos, et al., PTPN2 regulates interactions between macrophages and intestinal epithelial cells to promote intestinal barrier function, Gastroenterology 159 (2020) 1763-1777. https://doi.org/10.1053/j.gastro.2020.07.004.
[6] W.J. Yang, Y.Z. Cong, Gut microbiota-derived metabolites in the regulation of host immune responses and immune-related inflammatory diseases, Cell Mol. Immunol. 18 (2021) 866-877. https://doi.org/10.1038/s41423-021-00661-4.

[7] P. Zhang, Influence of foods and nutrition on the gut microbiome and implications for intestinal health, Int. J. Mol. Sci. 23 (2022) 9588. https://doi.org/10.3390/ijms23179588.

[8] S.J. Wu, Z.F. Bhat, R.S. Gounder, et al., Effect of dietary protein and processing on gut microbiota-a systematic review, Nutrients 14 (2022) 453. https://doi.org/10.3390/nu14030453.

[9] M.X. Ying, Q. Yu, B. Zheng, et al., Cultured *Cordyceps sinensis* polysaccharides modulate intestinal mucosal immunity and gut microbiota in cyclophosphamide-treated mice, Carbohydr Polym. 235 (2020) 115957. https://doi.org/10.1016/j.carbpol.2020.115957.

[10] X.J. Huang, S.P. Nie, M.Y. Xie, Interaction between gut immunity and polysaccharides, Crit. Rev. Food Sci. Nutr. 57 (2017) 2943-2955. https://doi.org/10.1080/10408398.2015.1079165.

[11] G.X. Ma, H.J. Du, Q.H. Hu, et al., Health benefits of edible mushroom polysaccharides and associated gut microbiota regulation, Crit. Rev. Food Sci. Nutr. 62 (2022) 6646-6663. https://doi.org/10.1080/10408398.2021.1903385.

[12] X. Wang, Y.H. Qu, Y. Wang, et al., *β*-1,6-Glucan from *Pleurotus eryngii* modulates the immunity and gut microbiota, Front Immunol. 13 (2022) 859923. https://doi.org/10.3389/fimmu.2022.859923.

[13] Y.X. Wang, T. Zhang, Y. Xin, et al., Comprehensive evaluation of alkali-extracted polysaccharides from *Agrocybe cylindracea*: comparison on structural characterization, Carbohydr. Polym. 255 (2021) 117502. https://doi.org/10.1016/j.carbpol.2020.117502.

[14] D.J. Hu, K.L. Cheong, J. Zhao, et al., Chromatography in characterization of polysaccharides from medicinal plants and fungi, J. Sep. Sci. 36 (2013) 1-19. https://doi.org/10.1002/jssc.201200874.

[15] J.Y. Huo, Z.Y. Wu, W.Z. Sun, et al., Protective effects of natural polysaccharides on intestinal barrier injury: a review, J. Agric. Food Chem. 70 (2022) 711-735. https://doi.org/10.1021/acs.jafc.1c05966.

[16] B. Wang, L.L. Yan, S.C. Guo, et al., Structural elucidation, modification, and structure-activity relationship of polysaccharides in Chinese herbs: a review, Front.Nutr. 9 (2022) 908175. https://doi.org/10.3389/fnut.2022.908175.

[17] T. Zhao, M. Yang, L.N. Ma, et al., Structural modification and biological activity of polysaccharides, Molecules 28 (2023) 5416. https://doi.org/10.3390/molecules28145416.

[18] M. Locati, G. Curtale, A. Mantovani, Diversity, mechanisms, and significance of macrophage plasticity, Annu. Rev. Pathol. 15 (2020) 123-147. https://doi.org/10.1146/annurev-pathmechdis-012418-012718.

[19] Y.Y. Du, L. Rong, Y.H. Cong, et al., Macrophage polarization: an effective approach to targeted therapy of inflammatory bowel disease, Expert. Opin. Ther. Targets. 25 (2021) 191-209. https://doi.org/10.1080/14728222.2021.1901079.

[20] M. Lee, E.B. Chang, Inflammatory bowel diseases (IBD) and the microbiome-searching the crime scene for clues, Gastroenterology 160 (2021) 524-537. https://doi.org/10.1053/j.gastro.2020.09.056.

[21] M.C. Mentella, F. Scaldaferri, M. Pizzoferrato, et al., Nutrition, IBD and gut microbiota: a review, Nutrients. 12 (2 020) 944. https://doi.org/10.3390/nu12040944.

[22] Y. Nie, Q.L. Lin, F.J. Luo, Effects of non-starch polysaccharides on inflammatory bowel disease, Int. J. Mol. Sci. 18 (2017) 1372. https://doi.org/10.3390/ijms18071372.

[23] X.Y. Liu, L.X. Wu, A.J. Tong, et al., Anti-aging effect of *Agrocybe aegerita* polysaccharide through regulation of oxidative stress and gut microbiota, Foods 11 (2022) 3783. https://doi.org/10.3390/foods11233783.

[24] Y. Ji, M.F. Zheng, S.G. Ye, et al., *Agrocybe aegerita* polysaccharide combined with chemotherapy improves tumor necrosis factor-alpha and interferon-gamma levels in rat esophageal carcinoma, Dis. Esophagus. 26 (2013) 859-863. https://doi.org/10.1111/j.1442-2050.2012.01397.x.

[25] Z.J. Zhu, R. Huang, A.H. Huang, et al., Polysaccharide from *Agrocybe cylindracea* prevents diet-induced obesity through inhibiting inflammation mediated by gut microbiota and associated metabolites, Int. J. Biol. Macromol. 209 (2022) 1430-1438. https://doi.org/10.1016/j.ijbiomac.2022.04.107.

[26] Q.D. Guan, A comprehensive review and update on the pathogenesis of inflammatory bowel disease, J. Immunol. Res. 2019 (2019) 7247238. https://doi.org/10.1155/2019/7247238.

[27] S. Mehandru, J.F. Colombel, The intestinal barrier, an arbitrator turned provocateur in IBD, Nat. Rev. Gastroenterol. Hepatol. 18 (2021) 83-84. https://doi.org/10.1038/s41575-020-00399-w.

[28] S.H. Lee, Intestinal permeability regulation by tight junction: implication on inflammatory bowel diseases, Intest. Res. 13 (2015) 11-18. https://doi.org/10.5217/ir.2015.13.1.11.

[29] T. Breugelmans, B. Oosterlinck, W. Arras, et al., The role of mucins in gastrointestinal barrier function during health and disease, Lancet. Gastroenterol. Hepatol. 7 (2022) 455-471. https://doi.org/10.1016/S2468-1253(21)00431-3.

[30] C.T. Capaldo, D.N. Powell, D. Kalman, Layered defense: how mucus and tight junctions seal the intestinal barrier, J. Mol. Med. (Berl). 95 (2017) 927-934. https://doi.org/10.1007/s00109-017-1557-x.

[31] Y.R. Na, M. Stakenborg, S.H. Seok, et al., Macrophages in intestinal inflammation and resolution: a potential therapeutic target in IBD, Nat. Rev. Gastroenterol. Hepatol. 16 (2019) 531-543. https://doi.org/10.1038/s41575-019-0172-4.

[32] X. Zhou, W.Y. Li, S. Wang, et al., YAP aggravates inflammatory bowel disease by regulating M1/M2 macrophage polarization and gut microbial homeostasis, Cell Rep. 27 (2019) 1176-1189 e1175. https://doi.org/10.1016/j.celrep.2019.03.028.

[33] S. Dharmasiri, E.M. Garrido-Martin, R.J. Harris, et al., Human intestinal macrophages are involved in the pathology of both ulcerative colitis and crohn disease, Inflamm. Bowel. Dis. 27 (2021) 1641-1652. https://doi.org/10.1093/ibd/izab029.

[34] L.L. Tian, J.L. Zhao, J.Q. Kang, et al., Astragaloside IV alleviates the experimental DSS-induced colitis by remodeling macrophage polarization through STAT signaling, Front. Immunol. 12 (2021) 740565. https://doi.org/10.3389/fimmu.2021.740565.

[35] C.Y. Huang, J. Wang, H.B. Liu, et al., Ketone body beta-hydroxybutyrate ameliorates colitis by promoting M2 macrophage polarization through the STAT6-dependent signaling pathway, BMC Med. 20 (2022) 148. https://doi.org/10.1186/s12916-022-02352-x.

[36] A.V. Vila, F. Imhann, V. Collij, et al., Gut microbiota composition and functional changes in inflammatory bowel disease and irritable bowel syndrome, Sci. Transl. Med. 10 (2018) 8914. https://doi.org/10.1126/scitranslmed.aap8914.

[37] R. Pittayanon, J.T. Lau, G.I. Leontiadis, et al., Differences in gut microbiota in patients with *vs.* without inflammatory bowel diseases: a systematic review, Gastroenterology 158 (2020) 930-946. https://doi.org/10.1053/j.gastro.2019.11.294.

[38] S. Stojanov, A. Berlec, B. Strukelj, The influence of probiotics on the Firmicutes/Bacteroidetes ratio in the treatment of obesity and inflammatory bowel disease, Microorganisms 8 (2020) 1715. https://doi.org/10.3390/microorganisms8111715.

[39] U. Gophna, K. Sommerfeld, S. Gophna, et al., Differences between tissue-associated intestinal microfloras of patients with Crohn's disease and ulcerative colitis, J. Clin. Microbiol. 44 (2006) 4136-4141. https://doi.org/10.1128/JCM.01004-06.

[40] T.P.N. Bui, L. Manneras-Holm, R. Puschmann, et al., Conversion of dietary inositol into propionate and acetate by commensal *Anaerostipes associates* with host health, Nat. Commun. 12 (2021) 4798. https://doi.org/10.1038/s41467-021-25081-w.

[41] Y.W. Wang, J.L. Song, Y. Zhai, et al., *Romboutsia sedimentorum* sp. nov., isolated from an alkaline-saline lake sediment and emended description of the genus *Romboutsia*, Int. J. Syst. Evol. Microbiol. 65 (2015) 1193-1198. https://doi.org/ 10.1099/ijs.0.000079.

[42] L. Boesmans, M. Valles-Colomer, J. Wang, et al., Butyrate producers as potential next-generation probiotics: safety assessment of the administration of *Butyricicoccus pullicaecorum* to healthy volunteers, mSystems 3 (2018) e00094-18. https://doi.org/10.1128/mSystems.00094-18.

[43] F.F. Wu, X.F. Guo, J.C. Zhang, et al., *Phascolarctobacterium faecium* abundant colonization in human gastrointestinal tract, Exp. Ther. Med. 14 (2017) 3122-3126. https://doi.org/10.3892/etm.2017.4878.

[44] N. Shi, N. Li, X.W. Duan, et al., Interaction between the gut microbiome and mucosal immune system, Mil. Med. Res. 4 (2017) 14. https://doi.org/10.1186/s40779-017-0122-9.

[45] H. Kayama, R. Okumura, K. Takeda, Interaction between the microbiota, epithelia, and immune cells in the intestine, Annu. Rev. Immunol. 38 (2020) 23-48. https://doi.org/10.1146/annurev-immunol-070119-115104.

[46] L.L. Liang, L. Liu, W.Y. Zhou, et al., Gut microbiota-derived butyrate regulates gut mucus barrier repair by activating the macrophage/WNT/ERK signaling pathway, Clin. Sci. (Lond). 136 (2022) 291-307. https://doi.org/10.1042/CS20210778.

[47] J. Ji, D.M. Shu, M.Z. Zheng, et al., Microbial metabolite butyrate facilitates M2 macrophage polarization and function, Sci. Rep. 6 (2016) 24838. https://doi.org/10.1038/srep24838.

[48] M.M. Sun, W. Wu, Z.J. Liu, et al., Microbiota metabolite short chain fatty acids, GPCR, and inflammatory bowel diseases, J. Gastroenterol. 52 (2017) 1-8. https://doi.org/10.1007/s00535-016-1242-9.

[49] P.V. Chang, L.M. Ha, S. Offermanns, et al., The microbial metabolite butyrate regulates intestinal macrophage function *via* histone deacetylase inhibition, Proc. Natl. Acad. Sci. USA. 111 (2014) 2247-2252. https://doi.org/10.1073/pnas.1322269111.